Published in the Proceedings of the 16th International Aluminum Alloys Conference (ICAA16) 2018
ISBN: 978-1-926872-41-4
by the Canadian Institute of Mining, Metallurgy & Petroleum

VOID EVOLUTION IN A 7XXX SERIES ALUMINUM ALLOY DURING HOT ROLLING: QUANTITATIVE EXPERIMENTAL RESULTS AND MECHANISM-BASED PROCESS SIMULATION

*G. Falkinger, G. Angerer, B. Gerold, and P. Simon

AMAG Rolling GmbH
Ranshofen, Austria
*(*Corresponding author: georg.falkinger@amag.at)*

ABSTRACT

This contribution presents an investigation of the evolution of shrinkage pores during hot rolling with a special focus on the microscopic mechanism. The reliable closure of pores, which inevitably occur during the casting process, is of crucial technological importance for high-quality hot rolled plate products. Therefore, lab-scale tests were carried out under different typical thermomechanical loadings. Extensive data from optical microscopy was collected before and after deformation. The analysis shows that the *average volume* of pores evolves similar to the volume of an idealized arrangement of voids in an ideally plastic matrix. The *average shape* of the shrinkage pores, however, was found to be almost constant during deformation. Even though individual pores exhibit complex morphologies far from any idealized geometries, the overall evolution of a large number of pores is well captured by simple assumptions. In addition to the quantitative analysis, a schematic representation of this counter-intuitive behavior is provided. A simple ‘Gurson’-type void evolution equation was implemented in a three-dimensional Finite-Element model of the industrial hot rolling process. With the help of this mechanism-based process simulation the thermomechanical closure of shrinkage pores during the rolling process has been optimized for a variety of plate products.

KEYWORDS

7xxx series aluminium alloy, Void closure model, Hot rolling

INTRODUCTION

Aluminum alloys of the 7xxx series are widely used in the aircraft industry. They have to meet high quality standards regarding microstructure as well as mechanical properties. For hot-rolled aircraft plates, one of the most important quality requirements is that they are free from pores. Pores, however, are inevitably created during the casting process either due to shrinkage or due to the dissolution of gas from the melt. The pores have to be closed mechanically during the hot-rolling process. Therefore, the mechanism of so-called pore closure or void closure has a high technological relevance for the production of aircraft plates.

The behaviour of voids in a ductile matrix subjected to mechanical deformation has been extensively studied, especially in the context of damage mechanics. A recent review (Besson et al., 2010) on modeling methods for ductile damage gives a good impression on how much experimental as well as theoretical effort has been dedicated to the problem of void evolution under mechanical loadings. Although void closure has been studied to a far lesser degree, it obeys to the same general theoretical evolution laws as void growth. The most basic theoretical result is that hydrostatic pressure drives void closure, while hydrostatic tension leads to void growth.

The mechanism of void closure depends on the void shape. This is illustrated by the example of a flat penny-shaped void, which under compression obviously closes much faster than a sphere with the same volume. Theoretical models have been developed for the evolution of simplified void geometries, such as spheres or cylinders (e.g. Gurson, 1977), spheroidal (Gologanu et al., 1997) and ellipsoidal voids (Ponte-Castaneda, 1994). In industrial cast ingots, however, the pores exhibit very complex morphologies, which are far from any idealized geometry. X-ray tomography revealed ‘tortuous’ voids in a 5xxx aluminium alloy (Chaijaruwanich et al., 2006).

The combined effect of mechanical deformation and diffusion on void growth has been extensively studied in the context of creep damage and many experimental as well as theoretical results exist (e.g. Van der Giessen et al., 1995). There are no corresponding systematic investigations regarding void closure. Diffusion, however, was found to affect void evolution at elevated temperatures and low deformation rates in a 5xxx series aluminum alloy (Chaijaruwanich et al., 2006). In contrast to pure mechanical closure, which is independent of temperature and strain rate, the contribution to void evolution due to diffusion is strongly time- and temperature-dependent.

The purpose of this work is to determine quantitative relations between void closure and mechanical loading under the conditions of industrial hot-rolling. Special emphasis is put on the role of void shape effects on the one hand and on the influence of diffusion on the other hand. Previous works investigated industrial loading conditions but were limited to artificial void geometries and arrangements (Wang et al., 1996, 2015). Realistic morphologies were investigated in (Chaijaruwanich et al., 2006). The rolling reductions as well as the strain rates however, were very low compared with industrial schedules.

In the above mentioned contributions, void closure was studied with the help of rolling experiments. The stress and strain path in such experiments is inhomogeneous and exact local values of stress and strain cannot be measured directly. This work employs uniaxial compression tests instead. Uniaxial compression tests are ideally suited for the present purpose of determining quantitative relations between void closure and mechanical loading, because the stress and strain path of the specimen are known exactly.

The rest of the paper is structured as follows: The first section presents the material, the compression test and the optical pore detection method. The second section summarizes the experimental results on void closure. On the basis of the present investigations the third section suggests a novel schematic mechanism for void closure. Furthermore results from the industrial hot-rolling simulation are shown in this section. The last section finally provides a summary of the main results and the conclusions.

EXPERIMENTAL METHODS

The material, which was used in this work is an aluminium alloy from the 7xxx series. Specimens were extracted from the center of the cast and homogenized ingot. The ingot was produced in a continuous casting process. Compression tests were performed on a Baehr DIL 805 quenching and deformation dilatometer. Cylindrical specimens with a diameter of 5 mm and a height of 10 mm were compressed isothermally and at constant strain rate. The bulk of the specimens deforms homogeneously under uniaxial compression. Only at strains exceeding 0.5 the specimen starts to bulge and deviations from the ideal uniaxial compression occur. In the center of the specimen the deviations are small and have been neglected. The stress triaxiality in uniaxial compression equals –1/3. Typical values for the hot rolling of thick plates are in the range between 0 to –1. After

deformation the samples were quenched to room temperature. Temperature, strain-rate and total strain vary according to Table 1. Three samples were tested for each variation. A wide range of strain-rates was chosen in order to determine a possible rate effect. The temperatures correspond to typical hot-rolling schedules of 7xxx alloys.

Table 1. Test matrix: Total strains, temperatures and strain rates

Total strain	Temperature [°C]	Strain-rate [s^{-1}]
0.5	380	0.005
	400	0.005
	425	0.005 / 0.05 / 0.5 / 1.0
1.0	425	0.005 / 0.05 / 0.5 / 1.0

For the optical microscopy, micro sections in parallel to the compression axis were prepared. The cylindrical specimens were grinded down to the specimen center and polished with magnesia. The sections were analyzed on an Olympus MX51 microscope with an automated x-y-z table. With the help of the automated table a series of consecutive pictures of the sample section was taken. The total area of the assembled pictures, which was analyzed on each sample, ranges from 20 to 30 mm^2, which yields a total area between 60 and 80 mm^2 for each test variation. Quantitative evaluation of the total area was carried out by means of the Olympus Stream Enterprise software. Voids with an equivalent diameter below 1 µm were discarded from the evaluation. Figure 1 and Figure 2 show a selected single picture and the assembly of a multitude of consecutive pictures, respectively.

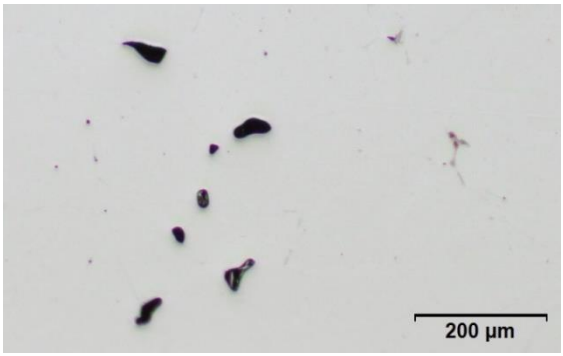

Figure 1. Micrograph of the cast and homogenized material with an agglomeration of pores (black) in the left half of the image.

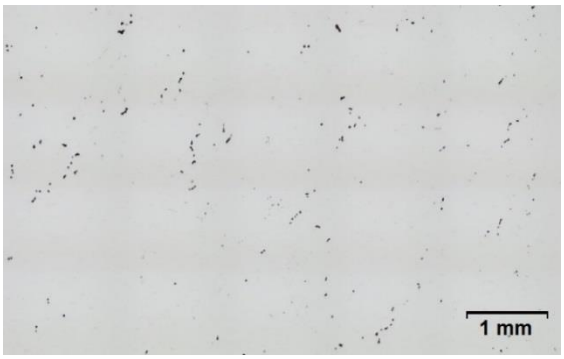

Figure 2. Assembly of micrographs of the cast and homogenized material. Assemblies with total areas ranging from 20 to 30 mm^2 for each specimen were used for the evaluation of voids.

In the following it is tacitly assumed that the measured void area fraction equals the actual void volume fraction. This is well justified for average values of void area but not for individual pores (Underwood, 1969). Due to their tortuous morphology, a large single pore might appear as two or more small pores in the two-dimensional section. The two-dimensional shape factor used in this paper to quantify the void morphology is the normalized ratio between the area and circumference of a single pore. For a circular void, the shape factor is normalized to equal 1.0. The two-dimensional shape factor does in general not equal its three-dimensional counterpart. Nevertheless the two-dimensional shape factor provides a good qualitative measure of the void shape and its evolution. For a three-dimensional characterization of void shapes in an aluminum alloy via X-ray tomography, see Chaijaruwanich et al. (2006).

EXPERIMENTAL RESULTS

In the cast and homogenized initial state, the material exhibits a void area fraction of 0.1714%. The void area fraction reduces to 0.022% at an equivalent strain of 0.5 and to 0.006% at an equivalent strain of 1.0. The sample sizes are six and four, respectively (cf. Table 1). Figure 3 shows the experimental results for all test variations. The values are normalized by the initial void area fraction. The error bars indicate the sample standard deviation and the dashed line connects the mean values. The figure shows the evolution of void area in dependence of total strain irrespective of temperature and strain rate

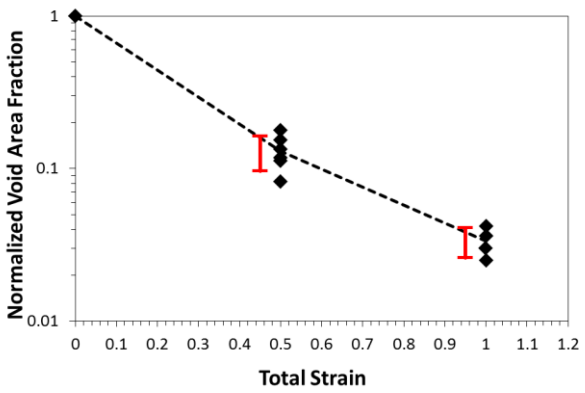

Figure 3. Void closure in dependence of strain in uniaxial compression tests. Dots: sample values; Dashed line: sample mean; Error bars: sample standard deviation.

The present results do not indicate any dependence of the void closure on temperature or on strain rate. The differences between the data points are attributed to statistical scatter. Figure 4 and Figure 5 show the results for compression tests at different strain rates and Figure 6 shows the results for the three tested temperatures. The mean value and the standard deviation represent the complete sample of test variations with the same total strain. A noteworthy contribution to void closure due to a diffusion based process can be excluded. Such a contribution would mark a clear trend towards increased void closure at low strain rates and high temperatures, which is not justified by the data.

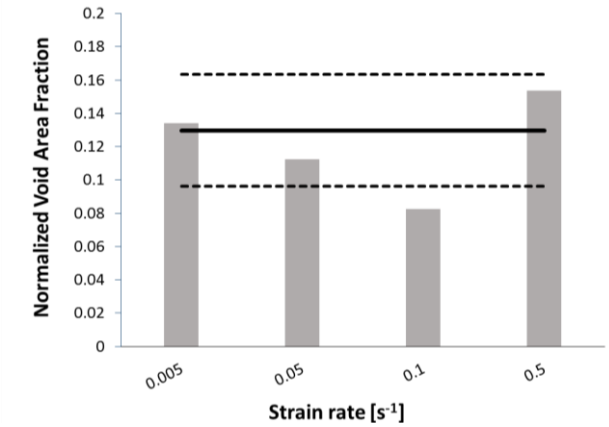

Figure 4. Void closure at a strain of 0.5 in dependence of strain-rate. Continuous line: sample mean value; Dashed line: sample standard deviation.

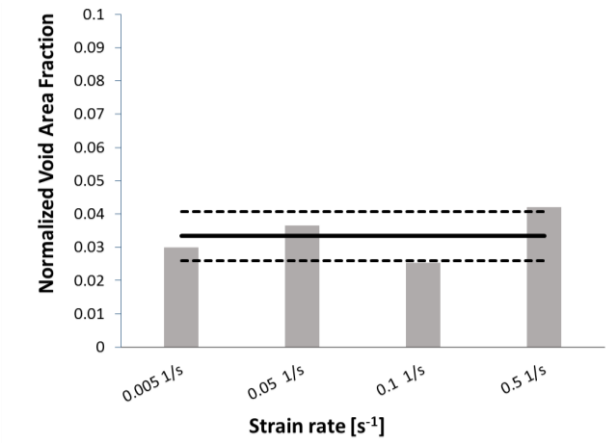

Figure 5. Void closure at a strain of 1.0 in dependence of strain-rate. Continuous line: sample mean value; Dashed line: sample standard deviation.

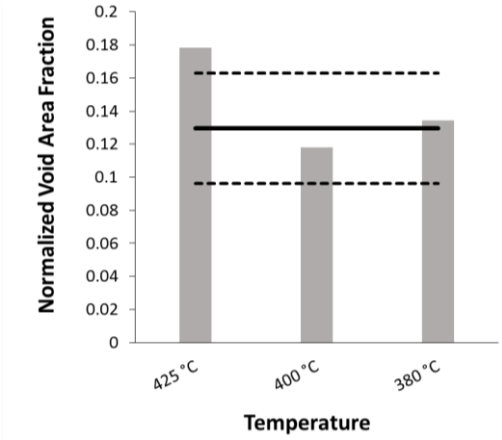

Figure 6. Void closure at a strain of 0.5 in dependence of temperature. Continuous line: sample mean value; Dashed line: sample standard deviation.

In the cast and homogenized ingot the pores assume very irregular and tortuous morphologies. This is reflected by an average two-dimensional shape factor of 0.68, which was determined in the undeformed state. Figure 7 shows the evolution of the shape factor with increasing strain. The average shape factor remains almost constant with mean values of 0.68 and 0.74 at strains of 0.5 and 1.0, respectively. This result strongly contrasts the idealized void closure mechanism of previous works (Stahlberg et al., 1980; Wang et al., 1996, 2015; Klung et al., 2012; Saby et al., 2015). In the idealized picture, regular spherical voids flatten out to penny- or needle-shaped ellipsoids. A more realistic schematic explanation of the underlying closure mechanism is suggested in the discussion section of this paper.

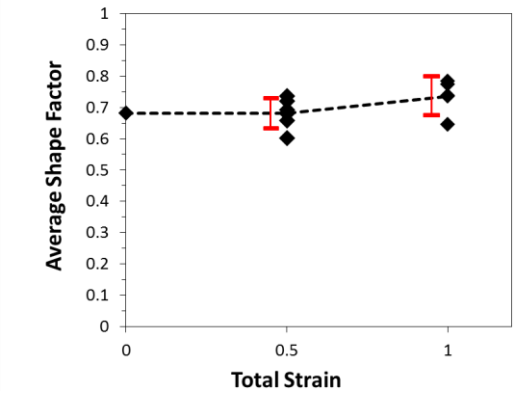

Figure 7. Evolution of the average two-dimensional shape factor in uniaxial compression tests. Dots: sample values; Dashed line: sample mean; Error bars: sample standard deviation.

DISCUSSION

Void Closure Mechanism

Starting with the work of (Stahlberg et al., 1980) many void closure models and laboratory experiments in the literature are based on the assumption that initially spherical or cubical voids deform to penny- or needle-shaped ellipsoids during void closure (Saby et al., 2015; Klung et al., 2012). This assumption is equivalent to a decreasing shape factor, which equals one for a sphere and tends to zero for flat ellipsoids. The present observation of a constant shape factor is irreconcilable with this idealized assumption. In order to provide a plausible explanation for the behaviour of the shape factor a simple alternative mechanism, schematically depicted in Figure 8, is suggested.

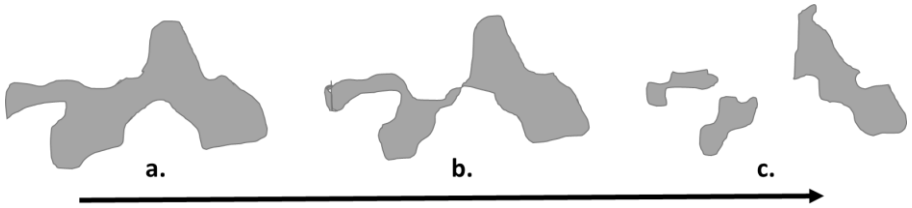

Figure 8. Schematic representation of the closure of tortuous voids. The initial void (a.) disintegrates into two (b.) and then three smaller voids (c.) under compression. The voids maintain irregular morphologies and the average void shape is constant.

Voids exhibit irregular tortuous morphologies already in the initial cast and homogenized state. The closure of individual pores is irregular as well, and during closure, single pores may disintegrate into again irregular smaller cavities. Hence, the shape factor of an individual pore may decrease or increase according to its individual shape and loading history. On average, however, there is no significant trend towards flattened shapes. On the contrary, if the conditions favor diffusion processes, Ostwald-ripening can even lead to the rounding of pores, and thus to an increasing shape factor (Chaijaruwanich et al., 2006).

A quantification of the effect of void shape evolution based on the Gologanu model (Gologanu et al., 1997) for spheroidal voids is given by Figure 9, where two cases are compared. The first case corresponds to the uniaxial compression of an initially spherical void to a penny-shaped void. In the second case an initially spherical void is compressed without shape change. The second case yields a good conservative estimate while the first leads to a different behaviour both qualitatively and quantitatively. This result is counter-intuitive: the simple model leads to far better results than the apparently more sophisticated one.

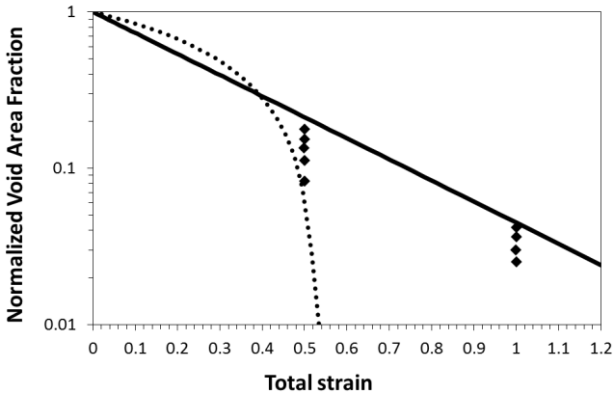

Figure 9. The effect of void shape evolution. Dashed line: Initial sphere flattened to penny-shaped ellipsoid. Continuous line: constant spherical shape. Dots: experimental values of this work.

Industrial Process Simulation

For the industrial hot-rolling simulation an evolution equation for spherical voids (Gurson, 1997) has been coupled to the Finite Element solver LS-Dyna. The amount of porosity is too small to affect the plastic behaviour of the material. Therefore, instead of the full model, a weak coupling between a J2-plasticity model and the evolution equation for the void volume has been employed. The equation reads as:

$$\dot{f} = qf\kappa\sinh(\kappa\eta)\dot{\varepsilon}$$

Here, f is the void volume fraction, η the stress triaxiality and ε the plastic equivalent strain. The parameter κ depends on the shape factor, for spherical voids it is equal to 3/2. The parameter q was introduced in order to take into account void interactions (Tvergaard, 1980). It was used as a calibration constant in this work. The calibration of the model is depicted in Figure 9. Details of the Finite Element model are presented elsewhere (Simon & Falkinger, 2016). An illustrative example of a three-dimensional rolling simulation is depicted in Figure 10. The initially homogenously distributed porosity vanishes after a rolling reduction of 90%. A trimming operation removes the residual porosity at the edge of the ingot. Considerable centerline porosity remains after smaller reductions of 40%. The simulation model is used to optimize rolling schedules and ingot dimensions, such as the initial thickness and the edge shape.

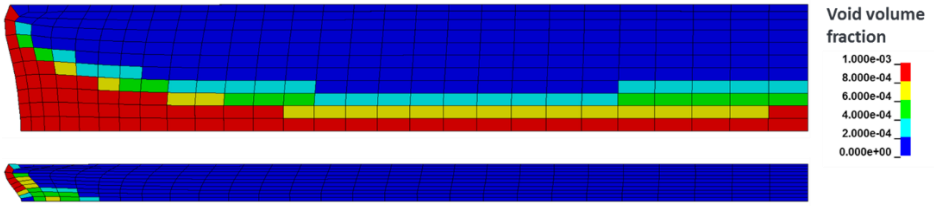

Figure 10. Simulation snap-shots of a quarter of the ingot cross-section after rolling reductions of 40% (upper picture) and 90% (lower picture), respectively. The center of the ingot is at the lower right corner of each simulation picture.

Figure 11 shows results from single pass rolling simulations. The ratio between rolled length and entry thickness determines the amount of void closure. In the center of the ingot, ratios greater than 0.6 are required to achieve substantial void closure. Low ratios below 0.3 induce void growth as a consequence of positive hydrostatic tension and should be avoided. The same ratio has been predicted by other authors (Chaijaruwanich et al., 2006). Accelerated void closure occurs closer to the surface of the ingot due to increased plastic deformation (Wang et al, 1996). A quantitative comparison between void closure at the center and at a quarter of the ingot thickness, as predicted by the simulation is shown in Figure 11.

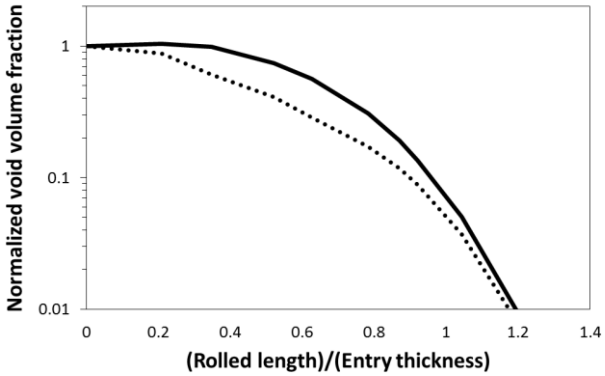

Figure 11. Void closure during hot rolling predicted by the simulation model. Continuous line: at the ingot center. Dashed line: at a quarter of the thickness.

CONCLUSIONS

The present investigation determined quantitative results for void closure of a 7xxx series aluminium alloy under industrial hot-rolling conditions. Well defined mechanical loadings at various strain rates and temperatures were applied to the cast and homogenized material with the help of compression tests. Regarding the mechanism of void closure, the following conclusions are made:

- There is no trend towards increased void closure at high temperatures or low strain-rates. A contribution of diffusion processes to the evolution of average void volume is therefore excluded.
- The average void shape is irregular at the beginning and remains irregular throughout deformation. The behaviour can be explained by a simple schematic representation.
- The simplified assumption of an initially spherical void, which deforms to a flat penny-shaped void contradicts the present results both quantitatively as well as qualitatively.

- Good agreement between experiment and theoretical model is achieved on the basis of constant spherical void shape.
- A simulation model coupled with the simple void evolution equation provides a formidable tool to optimize industrial rolling schedules with respect to void closure.

The results of this work are limited to average values of void volume and shape irrespective of void size. Void size-effects are beyond the scope of a two-dimensional analysis, due to the tortuous morphologies of the voids. Another limitation lies in the fact, that only one specific stress state, i.e. uniaxial compression, with a stress triaxiality of -1/3 could be created and analyzed. Actual values of the stress triaxiality in the rolling process of thick plates range from 0 to 1 and even higher values. The validation of the void closure model in the hot-rolling process is difficult due to the inhomogeneous deformation field across the ingot and requires further efforts.

REFERENCES

Besson, J. (2010). Continuum models of ductile fracture: A review. *Journal of Damage Mechanics, 19*, 1056–7895.

Chaijanuwarich, A., Dashwood, R.J., Lee, P.D., & Nagaumi, H. (2006). Pore evolution in a direct chill cast Al-wt.% Mg alloy during hot rolling. *Acta Materialia, 54*, 5185–5194.

Gologanu, M., Leblond, J.-B., Perrin, G., & Devaux, J. (1997). Recent extensions to Gurson's model for porous ductile metals. In P. Suquet (Ed.), *Continuum Microstructures* (pp. 61–130).

Gurson, A.L. (1977). Continuum theory of ductile rupture by void nucleation and growth: Part I – yield criteria and flow rules for porous ductile media. *Journal of Engineering Materials Technology, 99*(1), 2–15.

Klung, J.-S., Prakash, A., & Helm, D. (2012). Simulation of the void fraction evolution during hot rolling of a plastic mould stell ingot. *Procceedings of the International Conference of Ingot Casting, Rolling and Forging*, Aachen, Germany.

Ponte-Castaneda, P.P., & Zaidman, M. (1994). Constitutive models for porous media with evolving microstructure. *Journal of the Mechanics and Physics of Solids, 42*(9), 1459–1497.

Saby, M., Bouchard, P.-O., & Bernacki, M. (2015). Void closure criteria for hot metal forming: A review. *Journal of Manufacturing Processes, 19*, 239–250.

Simon, P., & Falkinger, G. (2017). Hot rolling simulation of aluminium alloys using LS-Dyna. *11th European LS-Dyna conference*. Salzburg, Austria. www.dynalook.com

Stahlberg, U., Keife, H., Lundberg, M., & Melander, A. (1980). A study of void closure during plastic deformation. *Journal of Mechanical Working Technology, 4*, 51-63.

Tvergaard, V. (1982). On localization in ductile materials containing spherical voids. *International Journal of Fracture, 18*, 237–252.

Underwood, E.E. (1969). Stereology, or the quantitative evaluation of microstructures. *Journal of Microscopy, 89*(2), 161–180.

Van der Giessen, E., Van der Burg, M.W.D., Needleman, A., & Tvergaard, V. (1995). Void growth due to creep and grain boundary diffusion at high triaxialities. *Journal of the Mechanics and Physics of Solids, 43*(1), 123–165.

Wang, A., Thomson, P.F., & Hodgson, P.D. (1996). A study of pore closure and welding in hot rolling processes. *Journal of Materials Processing Technology, 60*, 85–102.

Wang, B., Zhang, J., Xiao, C., Song, W., & Wang, S. (2015). Analysis of the evolution behavior of voids during the hot rolling process of medium plates. *Journal of Materials Processing Technology, 221*, 121–127.